

Reduction of Particle Reentrainment Using Porous Fence in Front of Dust Samples

Cheng-Hsiung Huang¹; Chin-I Lee²; and Chuen-Jinn Tsai³

Abstract: Wind tunnel experiments were conducted to measure the emission factor of particle reentrainment from a dust sample with or without a porous fence. The effect of wind velocity, fence porosity, and distance between the fence and the dust sample on the emission factor was studied. A 20% porous fence was found to be effective for reducing the particle reentrainment at a low wind velocity of 5 m/s. When the wind velocity was increased from 7 to 15 m/s, the results show that the particle reentrainment can also be reduced in a certain region behind the fence ($x/H < 4$, x =distance between fence and sample; H =fence height) for the 20% porous fence. A linear multivariable regression model was fitted to the logarithmically transformed experimental data. The good fit of the regression model makes it possible to estimate emission rate as a function of the dimensionless distance (x/H), the wind velocity, and the elapsed time.

DOI: 10.1061/(ASCE)0733-9372(2005)131:12(1644)

CE Database subject headings: Emissions; Porosity; Fences; Wind tunnels; Dust; Entrainment.

Introduction

The transportation of wind-blown particles has important environmental and health implications including transmission of disease, respiratory afflictions, and loss of soil nutrient. The Taiwan Environmental Protection Administration (Taiwan EPA) uses particulate matter less than 10 μm (PM_{10}) as an indicator of air quality. In addition, the mass concentrations of total suspended particle (TSP) and PM_{10} must meet the strict air quality standard promulgated by Taiwan EPA in April 1999. It is therefore of great importance to analyze the reduction of particles reentrainment from fugitive dust in order to develop effective methods for controlling the wind-blown particles.

The particle reentrainment of the road could come from the native soil or the redeposited dust from the entrainment particles. On soil surfaces, the particles will be emitted from the surface through abrasion by saltating grains. That is, when the wind velocity was slowly increased over the surface, the smaller or more exposed grains were entrained first by the air drag due to the influences of the surface creep or saltation. As the wind velocity rose, the larger grains were also moved by the air drag. Houser and Nickling (2001) used a series of wind tunnels on the clay-crust surface to examine the importance of saltation abrasion in the emission of PM_{10} . The results showed that the abrasion effi-

ciency (PM_{10} emission rate/saltation transport rate) was related to the crust strength, the amount of surface disturbance, and the velocity of the saltating grains. However, the entrainment of PM_{10} by aerodynamic forces was inherently difficult due to the strong cohesive forces associated with the deposited dust within the surfaces resulting from the soil enrichment, organic matter, or soluble salts (Gillette 1977; Nickling and Ecclestone 1981; McKenna-Neuman et al. 1996). Previous studies also showed that a particle will roll and be reentrained from the surface when the rotational moment of the particle overcame the moment caused by the adhesive force between particles and surfaces (Kousaka et al. 1980). Matsusaka and Masuda (1996) concluded that most of the reentrained particles were formed into aggregates, which were reentrained more easily than the primary particle. Nicholson (1993) found that the resuspension rate, which was defined as the fraction of particle removed from the surface in unit time, was related to the particle size, particle shape, and wind velocity. When the wind velocity increased, the resuspension rate also increased. Matsusaka and Masuda (1996) found that the reentrainment flux increased with time elapsed in an accelerated flow, while it decreased in a steady state flow.

The application of a porous fence as an artificial barrier is one of the commonly used methods to reduce the speed of oncoming winds. A number of previous papers have investigated the shelter effect and the flow characteristics behind the porous fences (Raine 1977; Gandermer 1979; Perera 1981; Borges and Viegas 1988; Raju et al. 1988). Raine (1977) measured the flow characteristics downstream of fences of different permeability cases. Gandermer (1979) had tested the flow pattern and shelter effects in the different fences. Perera (1981) studied the effect of porous and permeable hole shapes of porous wind breaks on the velocity defect, reattachment length, and Reynolds shear stress in the near wake. He found that a separation bubble that formed behind the fence disappeared when the porosity was greater than 30%, and the shelter effect occurred at small porosity conditions. Raju et al. (1988) presented an experimental study on the drag and turbulence intensity characteristics of a turbulent boundary layer flow past porous fences. Borges and Viegas (1988) investigated the

¹Department of Environmental Engineering and Health, Yuanpei Univ. of Science and Technology, No. 306 Yuanpei St. Hsinchu 300, Taiwan (corresponding author). E-mail: chhuang@mail.yust.edu.tw

²Institute of Environmental Engineering, National Chiao Tung Univ., Hsinchu, Taiwan.

³Institute of Environmental Engineering, National Chiao Tung Univ., Hsinchu, Taiwan.

Note. Discussion open until May 1, 2006. Separate discussions must be submitted for individual papers. To extend the closing date by one month, a written request must be filed with the ASCE Managing Editor. The manuscript for this paper was submitted for review and possible publication on February 23, 2004; approved on April 6, 2005. This paper is part of the *Journal of Environmental Engineering*, Vol. 131, No. 12, December 1, 2005. ©ASCE, ISSN 0733-9372/2005/12-1644-1648/\$25.00.

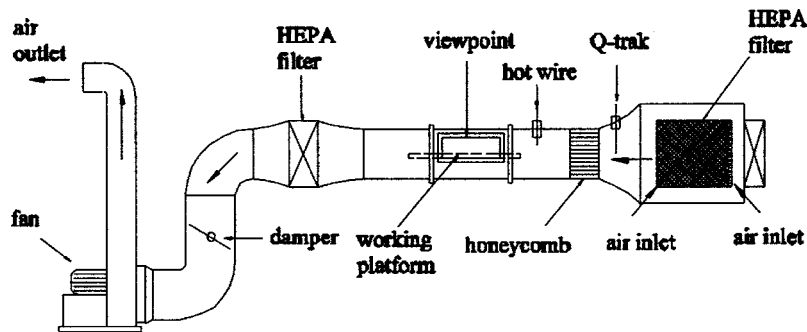


Fig. 1. Schematic representation of wind tunnel system

shelter effect of porous windbreaks by measuring the velocity and shear stress distribution behind these structures.

Several previous studies have investigated the flow structure behind various porous fences to find a good wind fence for abating wind-blown dusts. Fang and Wang (1997) simulated the turbulent flow around a vertical porous fence using a weakly compressible flow computational method. Results showed that as the fence porosity increases, the vortex tends to be elongated and results in a reduction of the drag on the fence. The drag force decreased with an increase of the boundary layer thickness of the approaching flow. Yaragal et al. (1997) conducted wind tunnel experiments under highly turbulent and disturbed flow conditions over a porous plate with a long splitter plate in its plane of symmetry. Their results showed that the fluctuating pressures were significantly dependent on the porosity of the porous plate. Shiau (1998) measured the turbulence characteristics for a turbulent boundary layer flow past the porous windscreen. Results show that the maximum Reynolds stress reduction along the downstream distance from the windscreen decays faster than the maximum mean wind speed reduction. The turbulence intensity profiles exhibit self preservation in the wake region of the windscreen for cases of 15, 30, and 50% porosity. Lee and Kim (1999) investigated experimentally the flow characteristics of the turbulent wake behind the porous fences. Among the porous fences used in their study, the porous fence with porosity of 20% shows the maximum reduction of mean streamwise velocity, but it has the highest vertical mean velocity at about $x/H=1$ location and large turbulence intensity in the near wake region. More recently, Lee et al. (2002) investigated experimentally the effect of porous wind fences on the wind erosion of sand particles from a two-dimensional triangular prism pile of sand. The results showed that sand particles begin to saltate and drift off from the sand pile surface when the wind speed approaches the threshold velocity. As the free stream velocity increases above the threshold velocity, the number of saltating particles rapidly increases. Sand particles with diameters ranging from about 150 to 330 μm were investigated in their study. To our knowledge, however, only few attempts have been undertaken that use small particles to examine the shelter effect of porous fences for preventing the particle re-entrainment from the dust sample.

In this study, a wind tunnel system was used to measure the emission factor of the reentrained particles with or without a porous fence in front of the test dust sample to examine the reduction performance of the porous fences. The effect of the wind velocity, porosity of porous fence, and distance between fences and dust samples on the emission factor was investigated. A linear multivariable regression was performed by fitting the experimental data using the least square estimate technique.

Methods

Fig. 1 shows the wind tunnel system used in this study to simulate the reentrainment of particles from the dust sample surface behind the porous fence at different wind velocities. The wind tunnel system includes a front HEPA filter, a honeycomb, a working platform, a back HEPA filter, and an exhaust fan. The outside air passes through the front HEPA filters before entering the contracted section. The filtered air then enters the honeycomb with a diameter of 30 cm, a length of 20 cm, and a tube diameter of 0.6 cm to smooth the air flow. The air flow passes the test dust sample inside the working platform having a length of 60 cm and a diameter of 30 cm, as shown in Fig. 2. A flat plate 0.3 cm thick constitutes the working platform. An aluminum cell with a cavity of 5 cm (length) \times 5 cm (width) \times 0.2 cm (depth) was used to contain the dust samples and was embedded in the flat plate. The front edge of the working platform was smoothed to prevent flow separation. A fence was installed downstream from the front edge of the working platform, also shown in Fig. 2. A schematic of the fence used in this study is shown in Figs. 3(a–c). The height, width, and thickness of the fence were 3.6, 20, and 0.7 cm, respectively. Circular holes in the porous fences were uniformly punctured and they had the geometric porosity (open area percentage) of $\epsilon=0\%$ (solid fence), 20 and 40%, respectively. In the wind tunnel system, another HEPA filter is installed downstream of the working platform to prevent the suspended particles from entering the exhaust fan. The exhaust fan has a frequency inverter to control the rotational speed of the motor. The inverter can regulate the air linear acceleration rate to a prescribed maximum wind velocity. The linear acceleration rate was fixed at 1.5 m/s^2 to speed up the air velocity from the calm wind to the maximum

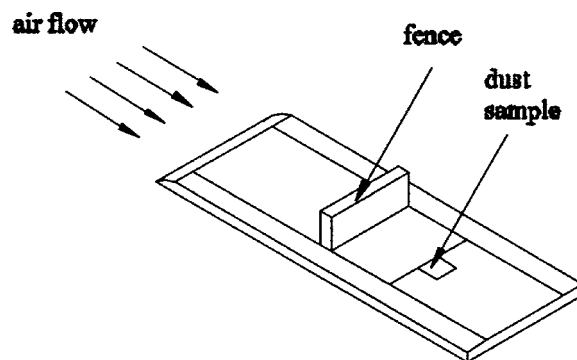


Fig. 2. Diagram of working platform with fence for test sample

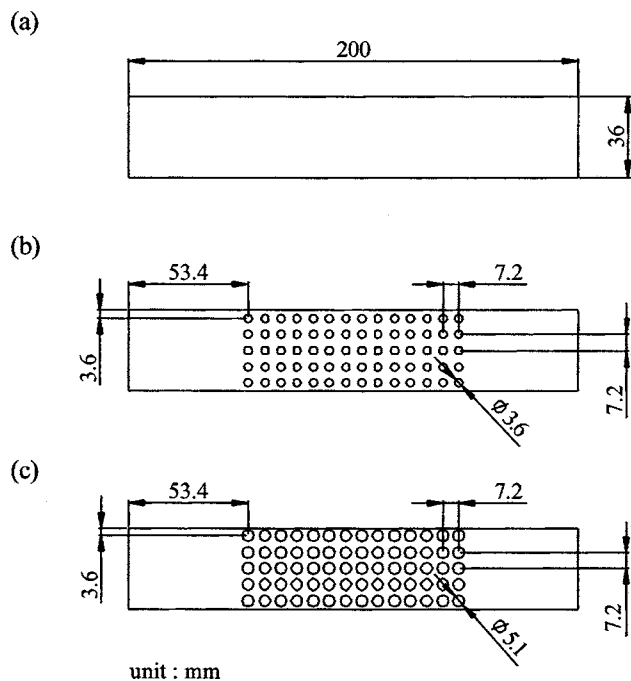


Fig. 3. Schematic of fence with porosity of: (a) $\varepsilon=0\%$ (solid fence), (b) $\varepsilon=20\%$, and (c) $\varepsilon=40\%$

wind velocity in this test. During the test, air temperature was from 23 to 27°C, and the relative humidity was between 55 and 70%.

Test dust samples were collected using a vacuum cleaner from an unpaved road at Nan Laio area in Hsin-Chu, Taiwan. The collected dust samples were sealed and transported to the laboratory. An oven was used to dry the dust samples at 105°C for 24 h. The dried dust samples were sieved using a standard Number 325 mesh to remove particles greater than 44 μm . The (MOUDI) microorifice uniform deposit impactor, Model 100, MSP, Minneapolis, Minn. was used to determine the initial and the reentrained size distribution of the dust samples, which were dispersed by the dust feeder (Wright Dust Feeder, WDF-II, BGI, Waltham, Mass.). Table 1 shows the particle distribution and the ratio of the initial and reentrained dust samples. This table tells us that the particles greater than 10 μm in aerodynamic diameter constituted the

Table 1. Particle Distribution and Ratio of Initial and Reentrained Dust Samples

Particle size (μm)	Initial		Reentrained	
	mass (μg)	Percentage (%)	mass (μg)	Percentage (%)
18–29.1	2,736,859	76.85	2,564	79.66
10–18	525,292	14.75	415	12.9
5.6–10	87,252	2.45	63	1.97
3.2–5.6	67,665	1.9	60	1.85
1.8–3.2	62,323	1.75	29	0.9
1.0–1.8	39,174	1.1	29	0.9
0.56–1.0	17,807	0.5	58	1.81
0.32–0.56	14,245	0.4	—	—
0.18–0.32	8,903	0.25	—	—
<0.053	—	—	—	—

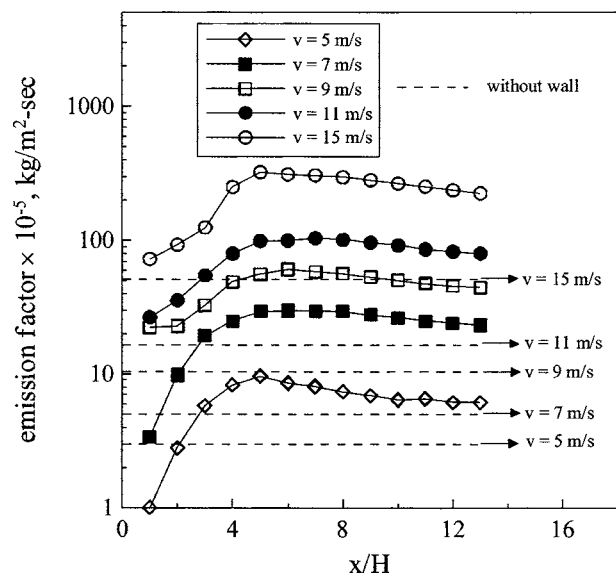


Fig. 4. Influence of distance between fence and dust sample on emission factor without and with solid fence at different wind velocities

major fraction of the dust samples and were found to be 91.6 and 92.6% of the total mass for the initial dust sample and the reentrained particles, respectively.

After the dust sample was put into the aluminum cell, the surface was flattened with a sharp knife edge. The aluminum cell containing the test sample was dried for 10 min and cooled for 5 min before being weighed. The test sample was reentrained on the working platform in the wind tunnel system at different wind velocities. Reentrainment occurs in the first 20 s. After the reentrainment test, the test sample was dried, cooled, and weighed again. The emission factor, E ($\text{kg}/\text{m}^2 \text{s}$) and emission rate, Λ (L/s) can be calculated as

$$E = (W_2 - W_1)/AT \quad (1)$$

$$\Lambda = (W_2 - W_1)/W_1 T \quad (2)$$

where W_1 (kg) and W_2 (kg)=mass of the test sample before and after reentrainment test, respectively; A (m^2)=surface area of the test sample; and T (s)=sampling time.

Results and Discussion

The emission factors of dust samples downstream from the solid and porous fence for various wind speeds were measured at different distances between fences and dust samples. Fig. 4 shows the emission factor of the test sample without and with solid fences for the different wind velocities at the air acceleration rate of 1.5 m/s^2 . The figure shows that the emission factor increases as the wind velocity is increased. When the distance behind the fence, x/H , is less than 4, the emission factor increases as the distance is increased and reaches a constant about 6.2, 25.1, 44.4, 79.8, and $224.8 \times 10^{-5} \text{ kg}/\text{m}^2 \text{ s}$ for the wind velocities of 5, 7, 9, 11, and 15 m/s , respectively. Compared to the case of the solid fence, the emission factor of the test sample without the fence (broken line) was found to be 3.0, 5.0, 10.4, 16.6, and $51.0 \times 10^{-5} \text{ kg}/\text{m}^2 \text{ s}$ for the wind velocities of 5, 7, 9, 11, and 15 m/s , respectively. It is seen that the emission factors of the test sample with the solid fence were much greater than those without the

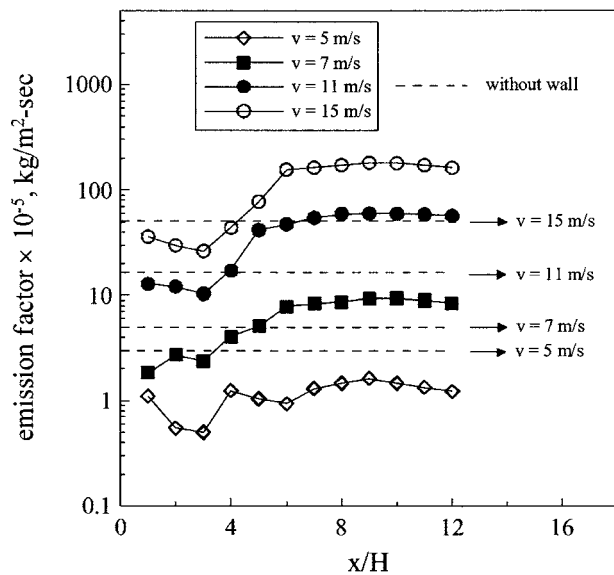


Fig. 5. Influence of distance between fence and dust sample on emission factor without and with porous fence of porosity $\varepsilon=20\%$ at different wind velocities

fence excluding the $x/H=0.5$ location for the wind velocities of 5 and 7 m/s. This indicates that the solid fence is ineffective at reducing particle reentrainment for the different wind velocities and the different distances behind the fence. This is due to the existence of the recirculating region just behind the solid fence which increases the possibility of the dust reentrainment.

On the contrary, for the $\varepsilon=20\%$ porous fence, as shown in Fig. 5, the emission factor of the test sample with the fence were smaller than those without the fence at low velocity ($v=5$ m/s), indicating it is useful to reduce particle reentrainment from the test sample. As the wind velocity increases up to 7, 11, and 15 m/s, this figure also shows that the porous fence is effective at reducing particle reentrainment in the region behind the porous fence ($x/H < 4$). This may be attributed to the reduction of the wind velocity penetrating the porous fence. As the flow proceeds in the downstream direction, beyond $x/H=4$, the emission factor of the test sample was increased and the porous fence could not reduce the particle reentrainment. Similar trends can also be seen in the case of the $\varepsilon=40\%$ porous fence. Fig. 6 shows that the emission factors of the test sample with the porous fence were greater than those without the fence for wind velocities of 7, 11, and 15 m/s. This indicates that the porous fence is not effective at reducing particle reentrainment for these wind velocities, while it has a modest reduction performance on particle reentrainment at wind velocities of 5 m/s.

To assist in the interpretation of the obtained results, a linear multivariable regression was performed for the $\varepsilon=20\%$ porous fence. Three parameters were used: the dimensionless distance behind the fence x/H ; the wind velocity U_0 (m/s); and time since the windflow began t (s). The emission rate Λ (L/s) was assumed to vary either in power law relationships or exponential relationships with the parameters and it can be expressed as

$$\log \Lambda = a + b \log \left(\frac{x}{H} \right) + c \log U_0 + d \log t \quad (3)$$

The regression analysis was conducted by fitting the equation to the experimental data of the $\varepsilon=20\%$ porous fence at the various wind velocities and the distances between fences and dust

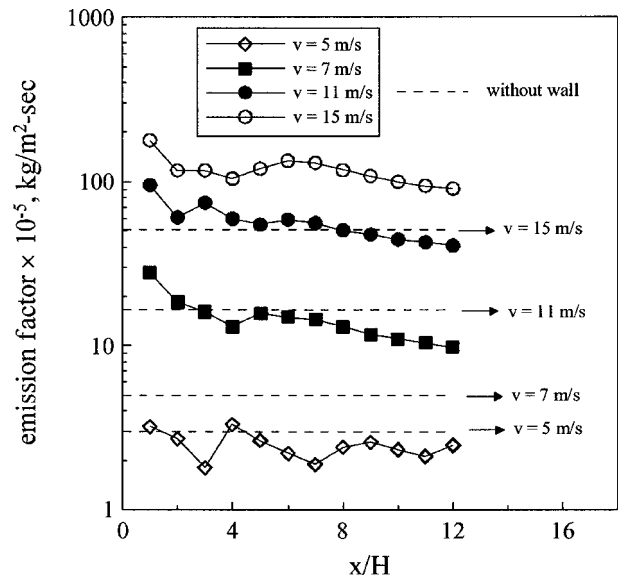


Fig. 6. Influence of distance between fence and dust sample on emission factor without and with porous fence of porosity $\varepsilon=40\%$ at different wind velocities

samples using the least square estimate technique. The results from the linear multivariable regression are given by the following equation:

$$\Lambda = 1.03015 \left(\frac{x}{H} \right)^{1.12111} U_0^{4.18759} t^{-3.35847} \quad (4)$$

In Fig. 7 we show that the emission rates obtained from the theoretical equation plotted against those measured by the experiment in the wind tunnel. The emission rates determined by the theory and by the experiment were highly correlated with R^2 of 0.986. The mean ratios of theoretical and experimental emission rate are close to 1, indicating the values are in agreement. Thus, the linear regression produced a good fit to the logarithmically transformed experimental data. It is possible to produce a mean-

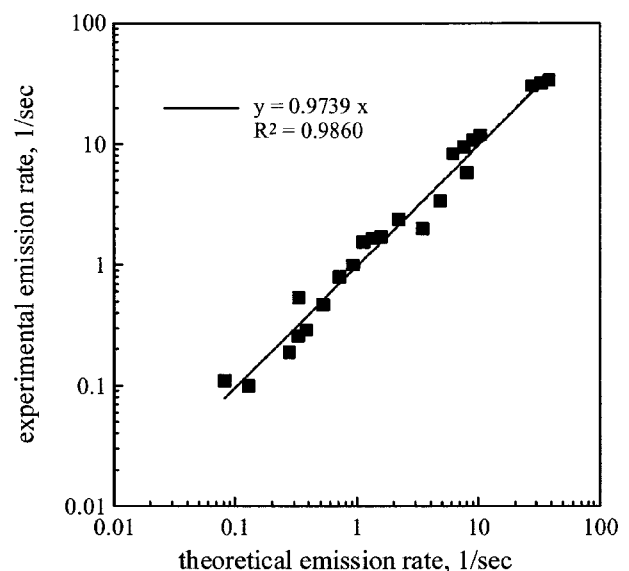


Fig. 7. Comparison of experimental emission rate with theoretical emission rate of dust sample for fence of porosity $\varepsilon=20\%$

ingful method to estimate the emission rate of the test dust sample behind the porous fence as a function of the dimensionless distance, the wind velocity, and elapsed time.

Conclusions

In this study, effects of wind velocity, fence porosity, and distance between the fence and the dust sample on the emission factor were investigated with or without the porous fence in the wind tunnel system. The results show that the emission factor with the solid fence is much greater than that without the solid fence at the same wind velocity, indicating the solid fence is ineffective at reducing particle reentrainment for the different wind velocities. However, for the $\varepsilon=20\%$ porous fence, the emission factors of the test sample with the porous fence were smaller than those without the porous fence at the low velocity of 5 m/s, indicating it is useful to reduce particle reentrainment from the test sample. As the wind velocity increases up to 7, 11, and 15 m/s, the $\varepsilon=20\%$ porous fence is still effective at reducing particle reentrainment in the region behind the porous fence ($x/H < 4$). A linear multivariable regression model was proposed by a good fit to the logarithmically transformed experimental data. The approach presented in this paper will be useful for reducing the particle reentrainment and estimating the emission rate of the dust samples.

Acknowledgments

The writers would like to thank the Taiwan National Science Council of the Republic of China for financial support under Contract No. NSC-89-EPA-Z-009-002.

References

- Borges, A. R., and Viegas, D. X. (1988). "Shelter effect on a row of coal piles to prevent wind erosion." *J. Wind. Eng. Ind. Aerodyn.*, 29, 145–154.
- Fang, M. F., and Wang, D. Y. (1997). "On the flow around a vertical porous fence." *J. Wind. Eng. Ind. Aerodyn.*, 67, 415–424.
- Gandermer, J. (1979). "Wind shelters." *J. Ind. Aerodyn.*, 4, 371–389.
- Gillette, D. A. (1977). "Fine particle emission due to wind erosion." *Trans. Am. Soc. Agric. Eng.*, 20, 891–897.
- Houser, C. A., and Nickling, W. G. (2001). "The factors influencing the abrasion efficiency of saltating grains on a clay-crusting playa." *Earth Surf. Processes Landforms*, 26, 491–505.
- Kousaka, Y., Okuyama, K., and Endo, Y. (1980). "Reentrainment of small aggregate particles from a plane surface by air stream." *J. Chem. Eng. Jpn.*, 13, 143–147.
- Lee, S. J., and Kim, H. B. (1999). "Laboratory measurements of velocity and turbulence field behind porous fences." *J. Wind. Eng. Ind. Aerodyn.*, 80, 311–326.
- Lee, S. J., Park, K. C., and Park, C. W. (2002). "Wind tunnel observations about the shelter effect of porous fences on the sand particle movements." *Atmos. Environ.*, 36, 1453–1463.
- Matsusaka, S., and Masuda, H. (1996). "Particle reentrainment from a fine powder layer in a turbulent air flow." *Aerosol Sci. Technol.*, 24, 69–84.
- McKenna-Neuman, C., Maxwell, C. D., and Boulton, J. W. (1996). "Wind transport of sand surfaces crusted with photoautotrophic microorganisms." *Catena*, 27, 229–247.
- Nicholson, K. W. (1993). "Wind tunnel experiments on the resuspension of particle material." *Atmos. Environ.*, 27, 181–188.
- Nickling, W. G., and Ecclestone, M. (1981). "The effects of soluble salts on the threshold shear velocity of fine sand." *Sedimentology*, 28, 505–510.
- Perera, M. A. E. S. (1981). "Shelter behind two-dimensional solid and porous fences." *J. Wind. Eng. Ind. Aerodyn.*, 8, 93–104.
- Raine, J. K. (1977). "Wind protection by model fences in a simulated atmospheric boundary layer." *J. Ind. Aerodyn.*, 2, 159–180.
- Raju, R., Garde, R. J., Singh, S. K., and Singh, N. (1988). "Experimental study on characteristics of flow past porous fences." *J. Wind. Eng. Ind. Aerodyn.*, 29, 155–163.
- Shiau, B. S. (1998). "Measurement of turbulence characteristics for flow past porous windscreen." *J. Wind. Eng. Ind. Aerodyn.*, 74, 521–530.
- Yaragal, S. C., Ram, H. S. G., and Murthy, K. K. (1997). "An experimental investigation of flow fields downstream of solid and porous fences." *J. Wind. Eng. Ind. Aerodyn.*, 66, 127–140.